Received: 1 April 2021 | Revised: 23 August 2021 | Accepted: 25 August 2021

DOI: 10.1096/fj.202100539RR

THE FASEB JOURNAL

RESEARCH ARTICLE

Inhibition of autophagy rescues muscle atrophy in a LGMDD2 *Drosophila* model

Águeda Blázquez-Bernal[1,2,3] | **Juan M. Fernandez-Costa**[1,2,3] | **Ariadna Bargiela**[1,2,3] | **Ruben Artero**[1,2,3]

[1]Translational Genomics Group, University Institute for Biotechnology and Biomedicine (BIOTECMED), University of Valencia, Valencia, Spain

[2]Area of Metabolism and Organic Failure, Incliva Health Research Institute, Valencia, Spain

[3]Incliva-CIPF Joint Unit, Valencia, Spain

Correspondence
Ariadna Bargiela, Translational Genomics Group, University Institute for Biotechnology and Biomedicine (BIOTECMED), University of Valencia, Valencia, Spain.
Email: ariadna.bargiela@uv.es

Present address
Juan M. Fernandez-Costa, Institute for Bioengineering of Catalonia (IBEC), The Barcelona Institute of Science and Technology (BIST), Barcelona, Spain

Funding information
Asociacion Conquistando Escalones; Regional Government of Valencia | Conselleria d'Educació, Investigació, Cultura i Esport (Ministry of Education, Research, Culture and Sports)

Abstract

Limb-girdle muscular dystrophy D2 (LGMDD2) is an ultrarare autosomal dominant myopathy caused by mutation of the normal stop codon of the *TNPO3* nuclear importin. The mutant protein carries a 15 amino acid C-terminal extension associated with pathogenicity. Here we report the first animal model of the disease by expressing the human mutant *TNPO3* gene in *Drosophila* musculature or motor neurons and concomitantly silencing the endogenous expression of the fly protein ortholog. A similar genotype expressing wildtype *TNPO3* served as a control. Phenotypes characterization revealed that mutant *TNPO3* expression targeted at muscles or motor neurons caused LGMDD2-like phenotypes such as muscle degeneration and atrophy, and reduced locomotor ability. Notably, LGMDD2 mutation increase TNPO3 at the transcript and protein level in the *Drosophila* model Upregulated muscle autophagy observed in LGMDD2 patients was also confirmed in the fly model, in which the anti-autophagic drug chloroquine was able to rescue histologic and functional phenotypes. Overall, we provide a proof of concept of autophagy as a target to treat disease phenotypes and propose a neurogenic component to explain mutant TNPO3 pathogenicity in diseased muscles.

KEYWORDS

autophagy, chloroquine, *Drosophila melanogaster*, limb-girdle muscular dystrophy D2, muscle atrophy, transportin 3

1 | INTRODUCTION

Limb-Girdle Muscular Dystrophies (LGMD) are a group of genetic muscular disorders characterized by an imbalance between muscle wasting and regeneration. The main clinical features of this heterogeneous group include proximal muscle weakness with histological signs of progressive muscle degeneration.[1]

Abbreviations: ActD, Actinomycin D; CQ, chloroquine; C-terminal, carboxy-terminal; IFM, indirect flight muscles; LGMD, limb-girdle muscular dystrophies; LGMD1F, limb-girdle muscular dystrophy 1F; LGMDD2, limb-girdle muscular dystrophy D2; MHC, myosin heavy chain; RT, room temperature; SR proteins, serine and arginine-rich proteins; sTNPO3mut, transportin-3 mutated on a sensitized background interfering Tnpo-SR; sTNPO3wt, transportin-3 wild type on a sensitized background interfering Tnpo-SR; TNPO3, transportin-3; TNPO3mut, transportin-3 mutated; TNPO3wt, transportin-3 wild type.

LGMDs can be classified into either autosomal dominant or recessive forms, depending on the mode of inheritance; the estimated incidence among all forms is 1:100 000.[2] One subtype of dominant LGMD is type D2 (LGMDD2, formerly known as LGMD1F, or TNPO3-related),[3] which affects about 60 people worldwide (OMIM 608423). LGMDD2 was initially described in a large Italo-Spanish family with proximal limb-girdle muscle weakness affecting up to eight generations.[4–6] Clinically, LGMDD2 has widely varying age of onset (range, 1–58 years), progression (slow-moderate), and severity. Initially, severe weakness occurs in the pelvic girdle muscles, and in later stages this weakness and muscle degeneration progress to the shoulder muscles. Skeletal deformities such as scoliosis, arachnodactyly (with or without contractures), scapular winging, and calf hypertrophy are additional features in several clinical cases of LGMDD2. In addition, some LGMDD2 patients suffer dysphagia and dysarthria, and respiratory involvement has also been reported in the juvenile-onset severe phenotype.[4,7] Patient muscle histopathology shows variations in size and shape of myofibers, atrophic and hypertrophic fibers, presence of central nuclei, and predominance of type I fibers. At the ultrastructural level, LGMDD2 patient biopsies show cytoplasmic accumulation of myofibrillar proteins, such as myotilin, and cytoskeletal proteins, such as desmin.[4,7–9]

LGMDD2 is caused by heterozygous deletion of a single adenine nucleotide in the stop codon (c.2771delA) of *transportin 3* gene (*TNPO3*). This mutation causes a carboxy-terminal (C-terminal) extension of 15 amino acids, producing a protein of unknown function (TNPO3mut) that is co-expressed with wild-type TNPO3 (TNPO3wt).[9,10] Recently, in addition to the well-known Italo-Spanish family, two new families and a sporadic case of LGMDD2 caused by different mutations in *TNPO3* have been identified. Importantly, all mutations give rise to a common 14-amino-acid C-terminal extension, which plays a pathogenic role regardless of the mutation type that generates it.[6,9–14] TNPO3 is a Ran-GTP-dependent β-importin that binds to serine and arginine-rich proteins (SR proteins) through its C-terminal domain, transporting them from cytosol to the nucleus. SR proteins include essential splicing factors and proteins mainly involved in mRNA splicing and metabolism.[15,16] Furthermore, TNPO3 is a key factor in the HIV-1 infection process, through its interaction with viral integrase and capsid.[17,18] It has been demonstrated that TNPO3mut prevents HIV-1 infection in CD4+ T cells from LGMDD2 patients.[18] Recent studies have shown that TNPO3 could play a role in the proteomic network that myotubes build during myogenesis.[19] Despite this data, the role of TNPO3 in muscle and pathogenic mechanisms in LGMDD2 remains largely unknown.

In skeletal muscle biopsies of LGMDD2 patients, increased levels of p62 and LC3 and autophagosomes have been detected, indicating that autophagy is upregulated in this dystrophy.[8] Autophagy is a pro-survival mechanism as it eliminates toxic proteins and damaged organelles in the cell, but overactivation leads to alterations in protein homeostasis due to excess protein degradation, which contributes to muscular atrophy and cell death.[20,21] A study of this potential pathogenetic activation of autophagy could therefore yield important insights into the connection between TNPO3mut and the molecular phenotype of LGMDD2. *Drosophila* is commonly used as a human neuromuscular disease model due to the conservation of the musculoskeletal system and human muscle development processes.[22–28] Indeed, models of different LGMD subtypes in the fly have been described.[29,30] Human *TNPO3* has an ortholog in *Drosophila*, *Tnpo-SR* (or *Trn-SR*), which was previously reported to have the same localization properties as its human counterpart and to recognize human SR and *Drosophila* proteins, thus confirming that fly and human transportins are functional homologous proteins.[31] Accordingly, *Drosophila* could be an outstanding animal to investigate LGMDD2.

Here we report the first animal model of LGMDD2 in *Drosophila,* developed by transgenic expression of the human *TNPO3* c.2771delA mutation (*TNPO3mut*) combined with simultaneous silencing of fly *Tnpo-SR*. In adult fly, *TNPO3mut* expression in somatic muscle and motor neurons significantly reduced the mean area of the indirect flight (IFM) and abdominal muscles. This muscle size reduction was concomitant with decreased locomotor capacity, reduced median survival, and upregulated autophagic activity. The *Drosophila* model thus provides the characteristic clinical signs of LGMDD2 and displays the overexpression of TNPO3, according to determination performed in patient samples.[13] Moreover, drug inhibition of autophagy in adult muscles by potent drug CQ was sufficient to rescue muscle phenotypes in this model. Briefly, CQ blocks late-stage autophagy by impairing the fusion of autophagosomes with lysosomes. As a consequence, the formation of autolysosomes gets reduced and cargoes degradation.[32,33]

Our data thus show evidence of pathogenic activation of autophagy in the LGMDD2 model and identify this process as a potential target in TNPO3mut-induced muscle atrophy. Additionally, we propose CQ as a candidate drug against LGMDD2. Overall, these results shed light on LGMDD2 physiopathology and provide proof of principle to develop therapeutic strategies.

2 | MATERIALS AND METHODS

2.1 | *Drosophila* transgenics

UAS-TNPO3wt and *UAS-TNPO3mut* transgenes were based on the N-terminal HA-tagged TNPO3 cDNA constructs provided by Dr Nigro (Second University of Naples, Naples, Italy).[10] Both constructs were released from the pCS2+ plasmid by *Bam*HI/*Xba*I digestion and were subcloned into *Bgl*II/*Xba*I sites in the pUAST plasmid.[34] Next, *UAS-TNPO3wt* and *UAS-TNPO3mut* transgenes were subcloned into the pCa4B plasmid[34] using the *Bam*HI restriction site. The pCa4B plasmid contains the *attpB* sites, by which cloned constructions can be integrated into the *Drosophila* genome using the PhiC31 integrase. PCa4B-UAS-TNPO3 plasmids were sent to the transgenesis company BestGene Inc. (California, USA) for microinjection into y^1w^{67c23}*; P-CaryP-attp40* embryos.[35] Five transgenic lines were obtained for each construction, and all constructs were integrated into chromosome 2L in the 25C7 cytogenetic region to ensure the same cDNA expression level in all lines.

2.2 | *Drosophila* stocks and crosses

The y^1w^{1118}*, D42-Gal4*, *Act5C-Gal4*, *UAS-GFP, UAS-IR-bcd, UAS-IR-Tnpo-SR,* and *UAS-GFP:Atg8a* fly strains were obtained from the Bloomington Drosophila Stock Center (Indiana University Bloomington, IN, USA). The *MHC-Gal4* line was previously described in Garcia-Lopez et al.[22] The following stocks were generated by standard genetic crosses: *UAS-TNPO3wt; UAS-IR-Tnpo-SR* (abbreviated as *sTNPO3wt*) and *UAS-TNPO3mut; UAS-IR-Tnpo-SR* (abbreviated as *sTNPO3mut*) for the expression of normal and mutated human *TNPO3,* respectively, in a background where endogenous *Tnpo-SR* is silenced; and the line *MHC-Gal4>UAS-GFP:Atg8a* for specific GFP:Atg8a expression in muscle. The crosses were carried out at 25°C, but the offspring was reared at 29°C to boost Gal4/UAS system overexpression in a standard nutrient medium. For treatment with ActD (Actinomycin D, ~98%, A1410, Sigma-Aldrich, St. Louis, MO, USA), 1-day adult flies were collected in tubes containing regular chow supplemented with 50, 200, or 800 nM ActD or 0.1% DMSO as vehicle. For CQ treatment (Chloroquine diphosphate salt solid, ≥98%, C6628, Sigma-Aldrich, St. Louis, MO, USA), tubes containing food supplemented with 10 or 100 μM CQ were used. For compound experiments, flies were transferred to tubes containing supplemented fresh food every 2–3 days.

2.3 | RT-qPCR

Total RNA was isolated using TriReagent (Sigma-Aldrich, St. Louis, MO, USA) from three biological replicates of ten 15-day-old adult males per replicate ($n = 30$). RNA purity and concentration were determined using a NanoDrop 1000 (Thermo Scientific, Waltham, MA, USA). Total RNA (1 μg) was reverse transcribed using Superscript II Reverse Transcriptase (Invitrogen, Carlsbad, CA, USA). EvaGreen-based real-time qPCR (Solis BioDyne, Tartu, Estonia) was performed using a QuantStudio 5 Real-Time PCR System (Applied Biosystems, Foster City, CA, USA). *Rp49* and *Tub48B* were used as endogenous references. For specific primer sequences, see Table S1. All experiments included three biological samples and three technical replicates from each sample. Expression levels were normalized to the reference gene using the $2^{-\Delta\Delta Ct}$ method.[36]

2.4 | Western blotting

For total protein extraction, three replicates per genotype of 30 thoraces of adult males aged 15 days ($n = 90$) were homogenized in RIPA buffer (Pierce, Thermo Scientific, Waltham, MA, USA) plus a cocktail of protease inhibitors (cOmplete, Roche Applied Science, Penzberg, Germany). Total proteins were quantified with the BCA (Pierce, Thermo Scientific, Waltham, MA, USA) protein test kit using whey albumin as standard protein. A total of 40 μg of protein was denatured from each sample for 5 min at 100°C, separated into SDS-PAGE gels at 8% by electrophoresis, and transferred to nitrocellulose membranes of 0.45 μm (Amersham Protran, GE Healthcare Life Sciences, Pittsburgh, PA, USA). The membranes were blocked with 5% skimmed milk powder in PBS-T (Na_2HPO_4 8 mM, NaCl 150 mM, KH_2PO_4 2 mM, KCl 3 mM, Tween 20 to 0.1%, pH 7.4) for 1 h at room temperature (RT) and then incubated overnight at 4°C with the primary antibodies at the appropriate dilution in 5% blocking solution. Primary antibodies used for blotting were from mouse: anti-TNPO3 (1:50, Abcam, Cambridge, UK), anti-HA epitope tag (1:100, Sigma-Aldrich, Sant Luis, MO, USA), anti-GFP (1:1000, Sigma-Aldrich, Sant Luis, MO, USA), and anti-α-tubulin (1:500, Developmental Studies Hybridoma Bank, University of Iowa, IA, USA), as the loading control. Goat horseradish peroxidase (HRP)-conjugated anti-mouse-IgG (1:3500, Sigma-Aldrich, Sant Luis, MO, USA) was used as secondary antibody. Immunoreactive bands were detected by chemiluminescence using ECL Western Blotting Substrate or SuperSignal West Pico PLUS Chemiluminescent Substrate (Pierce, Thermo Scientific, Waltham, MA, USA), and images were acquired in an

ImageQuant LAS 4000 or Amersham ImageQuant 800 (GE Healthcare Life Sciences, Pittsburgh, PA, USA). Quantification was performed using ImageJ software (NIH).[37]

2.5 | Histological analysis

The IFM area of *Drosophila* thoraces was analyzed as previously described.[38,39] Briefly, six thoraces of adult females of each genotype, aged 7 and 15 days, were embedded in epoxy resin following standard procedures. After drying the resin, semi-thin cross sections of 1.5 μm were made using Reichert Jung Ultracut Ultramicrotome (Leica Microsystems, Wetzlar, Germany). Sections were stained with toluidine blue to enhance contrast, and images were taken at 100× magnification using a Leica DM2500 microscope (Leica Microsystems, Wetzlar, Germany). Six images of IFMs were taken per fly and converted into binary images to quantify the muscle area. ImageJ software (NIH)[37] was used to quantify the percentage of pixels corresponding to muscle tissue (IFMs, black pixels) out of the total.

2.6 | Fluorescence methods

Abdominal muscles were visualized with phalloidin in six 15-day-old female flies dissected by making a face-flow cut, which allows the heart and abdominal muscles to be exposed from the dorsal part of the fly, as previously described.[40] After fixing the flies with 4% paraformaldehyde (PFA) for 20 min at RT, three washes were performed using PBS-T (PBS with 0.3% Triton X-100), stained in darkness with phalloidin–tetramethylrhodamine B isothiocyanate (1:1000, Sigma-Aldrich, Sant Luis, MO, USA) prepared in PBS-T for 1 h at RT and washed three times with PBS. Preparations were assembled with fluorescence-mounting media (Dako, Glostrup, Denmark) and images were taken at 100× magnification using an LSM800 confocal microscope (Zeiss, Jena, Germany). Using ImageJ software (NIH),[37] three measurements were made of each A4 fiber width, one at each end of the fiber and one between those two points. The five A4 fibers closest to the heart were quantified from each fly.

For staining GFP, thoraces of between four and eight 15-day-old female flies were dissected and fixed in 4% PFA at 4°C overnight. Afterward, tissue was incubated in 30% sucrose for two days at 4°C. Next, thoraces were embedded in Optimal Cutting Temperature reagent (OCT, Tissue-Tek, Sakura Europe, The Netherlands), and longitudinal cryosections of 10 μm were obtained using a Leica CM 1510S cryostat (Leica Microsystems, Wetzlar, Germany). Staining was performed as previously described.[26,41] Images were acquired at 400× magnification using an LSM800 confocal microscope (Zeiss, Jena, Germany) using the following settings: scan direction: bidirectional; laser wavelength: FITC: 2%, DAPI: 1%, pinhole; FITC: 50 μm, DAPI: 50 μm detector gain; FITC: 750 V, DAPI: 650 V, detector offset; FITC: −100, DAPI: −100, detector gain; FITC: 1, DAPI: 1. Quantification of the signal corresponding to GFP in the images was performed using ImageJ software (NIH).[37] Briefly, an entire region of the muscle was determined in each acquired micrograph, using the ImageJ software. Then, the integrated density of the green channel (or FITC fluorophore) was obtained and normalized against muscle area. Three images, corresponding to three different fields of the fly thorax were analyzed from each individual with a minimum of four flies per condition.

For lysosomes detection in *Drosophila* muscles, tissue was prepared as previously described.[42] Thoraces were incubated for 30 min at 37°C LysoTracker RED-DND99 (Invitrogen, Carlsbad, CA, USA). After three washes with PBS, the tissue was incubated with 4% PFA 20 min at RT, washed thrice with PBS and mounted using fluorescence mounting medium with DAPI (Vectashield, Vector Laboratories, CA, USA). Images were taken at 400x magnification using an LSM800 confocal microscope (Zeiss, Jena, Germany).

2.7 | Functional assays

Using the protocol detailed in Babcock and Ganetzky,[43] flight assays were carried out using 80–100 15-day-old male flies per genotype.

A negative geotaxis test was performed to assess climbing speed.[41] Between twenty-five and thirty 15-day-old male flies of each genotype were used. After 24 h without anesthesia, flies were transferred to disposable pipettes (1.5 cm in diameter and 25 cm in height) in three groups of 10 flies. The height reached from the bottom of the pipette for each fly over a period of 10 s was recorded with a camera.

2.8 | Lifespan and eclosion assays

A total of 100 newborn male flies were collected per genotype, distributed in 25 flies per tube containing standard nutrient medium, and kept at 29°C. The flies were transferred to new tubes with fresh nutritive medium every other day, and deceased flies were quantified daily according to.[41]

The eclosion assay was carried out by adapting the reference protocol.[44] 25–30 larvae from the first late-stage/

second early stage were placed in tubes containing standard fly food or supplemented food, and their development was complete.

2.9 | Statistical analyses

All statistical analyses were performed using GraphPad Prism 7 software. *p*-Values were obtained using a two-tailed, non-paired *t*-test ($\alpha = .05$) for all data except survival curves, applying Welch's correction when variances were significantly different. Survival curves were obtained using the Kaplan–Meier method, and statistical analysis was performed using the standard log-rank method (Mantel–Cox) ($\alpha = .05$) and the Gehan–Breslow–Wilcoxon method ($\alpha = .05$), which gives more weight to deaths in the early days. The details for the statistical analysis used in each figure panel are described in figure legends.

3 | RESULTS

3.1 | Generation of the *Drosophila* model

LGMDD2 is best known via study of an Italian-Spanish family in which the origin was described as c.2771delA mutation in the *TNPO3* gene[6,9,10]; besides, three different mutations in TNPO3 causing LGMDD2 have recently been identified. Nonetheless, these new mutations cause a similar extension in the C-terminal domain of TNPO3, with 14 identical amino acids (Figure 1A), so they are predicted to play the same pathogenic role as c.2771delA.[6,10-14] Due to the dominant nature of LGMDD2 pathology, overexpression of the human TNPO3mut version of the protein was hypothesized to be sufficient to trigger similar muscular defects in the fly. To this end, two transgenic *Drosophila* were generated: one expressed a transgene with the c.2771delA mutant version of human *TNPO3* (*UAS-TNPO3mut*), and another expressed the wild type version (*UAS-TNPO3wt*) as control of the former. Each transgene was inserted into the same attP site, attp40 in chromosome 2, to standardize position effects. This genomic position was selected for its promotion of high expression levels.[26] Since LGMDD2 is a myopathy, we first targeted the expression of both *UAS-TNPO3* to the *Drosophila* muscles using the *Myosin heavy chain* (*MHC*)-*Gal4* driver and confirmed the expression of both transgenes in *Drosophila* thoraces. To check the *TNPO3* transgenes were correctly integrated, we detected TNPO3 expression by western blot with anti-TNPO3 and anti-HA, taking advantage of the tag fused to these proteins (Figure 1B). In flies that express *UAS-TNPO3mut* the size of the detected band was slightly greater than in flies expressing *UAS-TNPO3wt*, consistent with the 15-amino-acid C-terminal extension generated by the mutant stop codon present in LGMDD2 patients. Accordant with the specificity of the two antibodies, control flies not expressing any human transgenes were not immunoreactive. Importantly, quantification of the results revealed a significantly higher amount of TNPO3mut than the wild-type counterpart, suggesting that the mutant mRNA or protein were more stable, or mutant mRNA was more efficiently translated. Although *TNPO3mut* expression in fly muscle impaired locomotion and median survival in flies (Figure S1), it did not produce significant muscular atrophy in the *Drosophila* IFM. These fibrillary muscles with a very similar sarcomere organization to humans have been widely used to reproduce the muscle atrophy associated with human muscle diseases.[23,27] Indeed, TNPO3mut did not generate IFM degeneration in 1-, 3-, or 4-week-old flies (Figure S2), a critical phenotype in LGMDD2 patients. Thus, TNPO3mut appeared insufficient to trigger obvious pathogenic defects in *Drosophila*.

We reasoned that this might be because flies have a functional ortholog of *TNPO3*, *Tnpo-SR*,[31] which could rescue the pathogenicity of *TNPO3mut*. To test this hypothesis, we generated fly stocks that simultaneously expressed the *TNPO3wt* or *TNPO3mut* transgenes and a *Tnpo-SR* interfering construct by RNAi[45] under the control of the *MHC-Gal4* driver, hereafter abbreviated as *sTNPO3*wt and *sTNPO3mut*. To confirm *Tnpo-SR* silencing, we quantified its levels in flies expressing the RNAi under the *MHC-Gal4* driver and we confirmed around 50% of silencing (Figure S3A). Additionally, the reduction of *Tnpo-SR* expression was also functional, since in flies with the silenced gene showed a spectacular decrease in almost threefold in mean life, from 29 days in control flies to 10 in flies with the interfering construction. Concomitantly, lifespan was also significantly reduced after silencing endogenous *Tnpo-SR* (Figure S3B).

Thus, *sTNPO3wt* flies serve as controls both for effects of human protein overexpression and specificity of the human mutation. Along the same lines, we found that on a sensitized background, *TNPO3mut* expression increased transcript and protein levels in fly muscles compared to the *sTNPO3wt* flies (Figure 1C,D). To confirm that LGMDD2 mutation leads to TNPO3 accumulation in model flies, we inhibited mRNA synthesis by treating flies with Actinomycin D (ActD). Concisely, ActD is an inhibitor of DNA-dependent RNA polymerase through its binding to guanine residues.[46] ActD treatment of LGMDD2 model

(A)

	Peptide sequence
TNPO3 wild type	QVTSAEECKQ VCWALRDFTR LFR
c.2771delA	QVTSAEECKQ VCWALRDFTR LFRCSHSCTV PVTQECLF
c.2766delT	QVTSAEECKQ VCWALRDFTR LFDSSHSCTV PVTQECLF
c.2767delC	QVTSAEECKQ VCWALRDFTR LFDSSHSCTV PVTQECLF
c.2757delC	QVTSAEECKQ VCWALRDFTG CFDSSHSCTV PVTQECLF

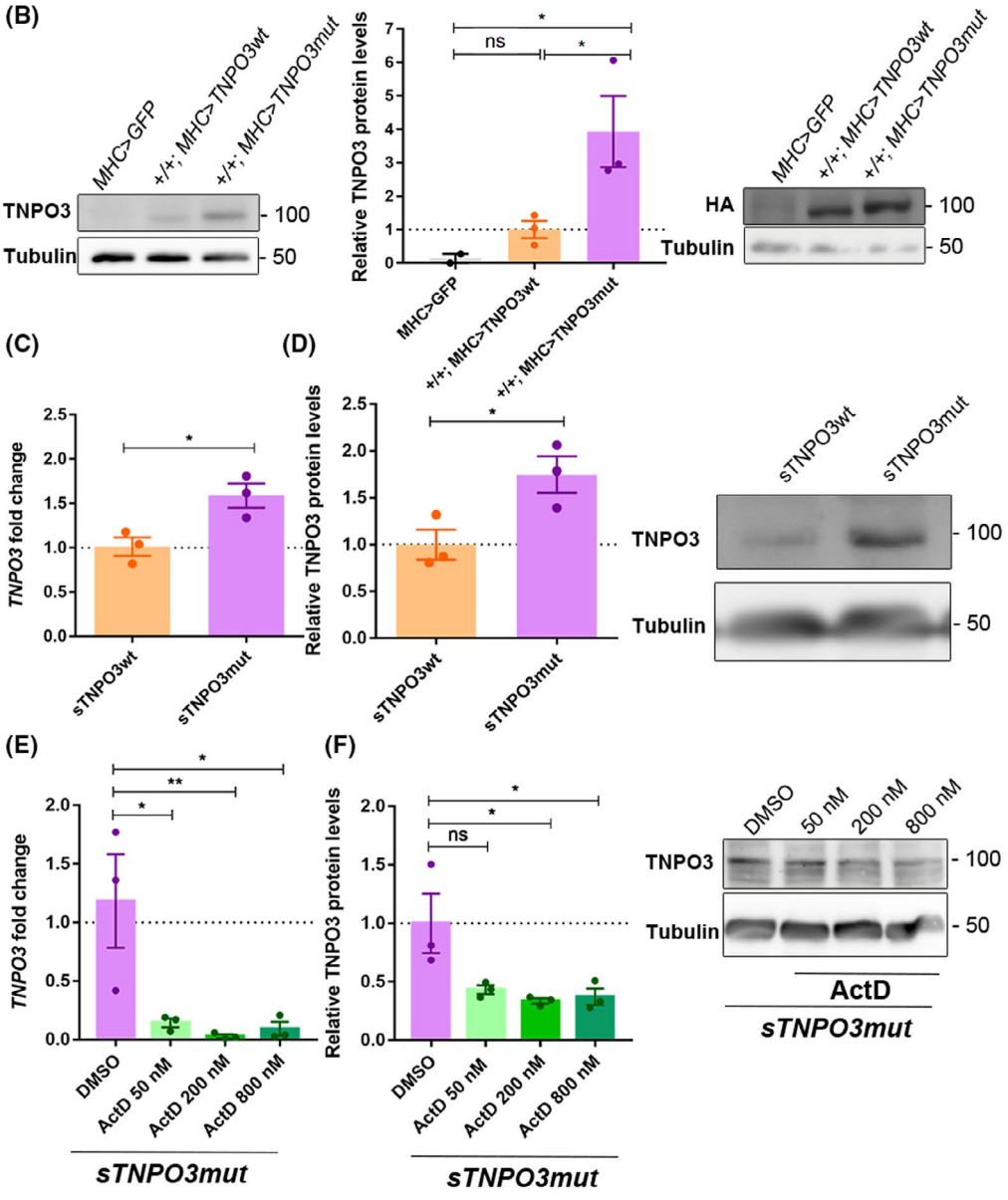

FIGURE 1 LGMDD2 model in *Drosophila melanogaster*. (A) Peptide sequence of wild type and different mutations in TNPO3 as described in Refs. [10–14] The wild-type sequence is indicated in black; purple sequence indicates the 14 amino acids conserved in all mutations and green marks new amino acids as a consequence of frameshift mutations. (B) Representative blots and quantification of TNPO3 and HA were performed using protein extracts from thoraces of control flies (*MHC-Gal4>UAS-GFP*), flies expressing wild-type TNPO3 (*MHC-Gal4>UAS-TNPO3wt*), and mutant TNPO3 flies (*MHC-Gal4>UAS-TNPO3mut*). Representative blots and quantification of human TNPO3 protein (C, E) and transcripts (D, F) in extracts from thoraces of *sTNPO3wt* (orange bars; *MHC-Gal4>UAS-TNPO3wt; UAS-IR-Tnpo-SR*) and *sTNPO3mut* (purple bars; *MHC-Gal4>UAS-TNPO3mut; UAS-IR-Tnpo-SR*) flies (C, D) and *sTNPO3mut* flies fed with 0.1% DMSO as vehicle or with the indicated concentrations of ActD for 15 days (E, F). In both cases, $n = 3$ or 4. α-Tubulin was used as an endogenous control to normalize protein levels. *TNPO3* is referenced to *Rp49* and *Tubulin* expression. The bar graphs show mean ± SEM. $^{*}p < .05$, $^{**}p < .01$ according to Student's *t*-test or one-way ANOVA test in E and F

flies reduce TNPO3 drastically at transcript and protein level (Figure 1E,F). Tus, suggesting that TNPO3mut favors mRNA and protein accumulation.

3.2 | Targeted expression of *TNPO3mut* to *Drosophila* muscle or motor neurons causes muscle atrophy and degeneration

LGMDD2 is primarily a muscle disease characterized by progressive muscle weakness and atrophy, but nervous system-related symptoms have also been described in patients.[4,7] Thus, after confirming the correct human *TNPO3* versions were expressed we targeted transgene expression to the fly muscle and motor neurons, with the *MHC-Gal4* and *D42-Gal4* drivers, respectively, maintaining a consistently *Tnpo-SR*-silenced background. Quantification of the cross-sectional muscle area of 7-day-old fly IFM expressing *TNPO3mut* in muscles (Figure 2A–D) or motor neurons (Figure 2E–H) showed no significant changes compared to *sTNPO3wt* flies and their control flies *(MHC-Gal4>UAS-GFP* and *D42-Gal4>UAS-GFP,* respectively). At 15 days old, however, the total IFM area of flies expressing *TNPO3mut* decreased significantly compared to controls in muscles (27% reduction) (Figure 3A–D) and motor neurons (23% reduction) (Figure 3E–H). Expression of *TNPO3wt* in the somatic muscles of 15-day-old flies also caused a significant reduction in muscle area compared to control flies, but less than the muscle atrophy brought about by *TNPO3mut*. Therefore, the muscle atrophy

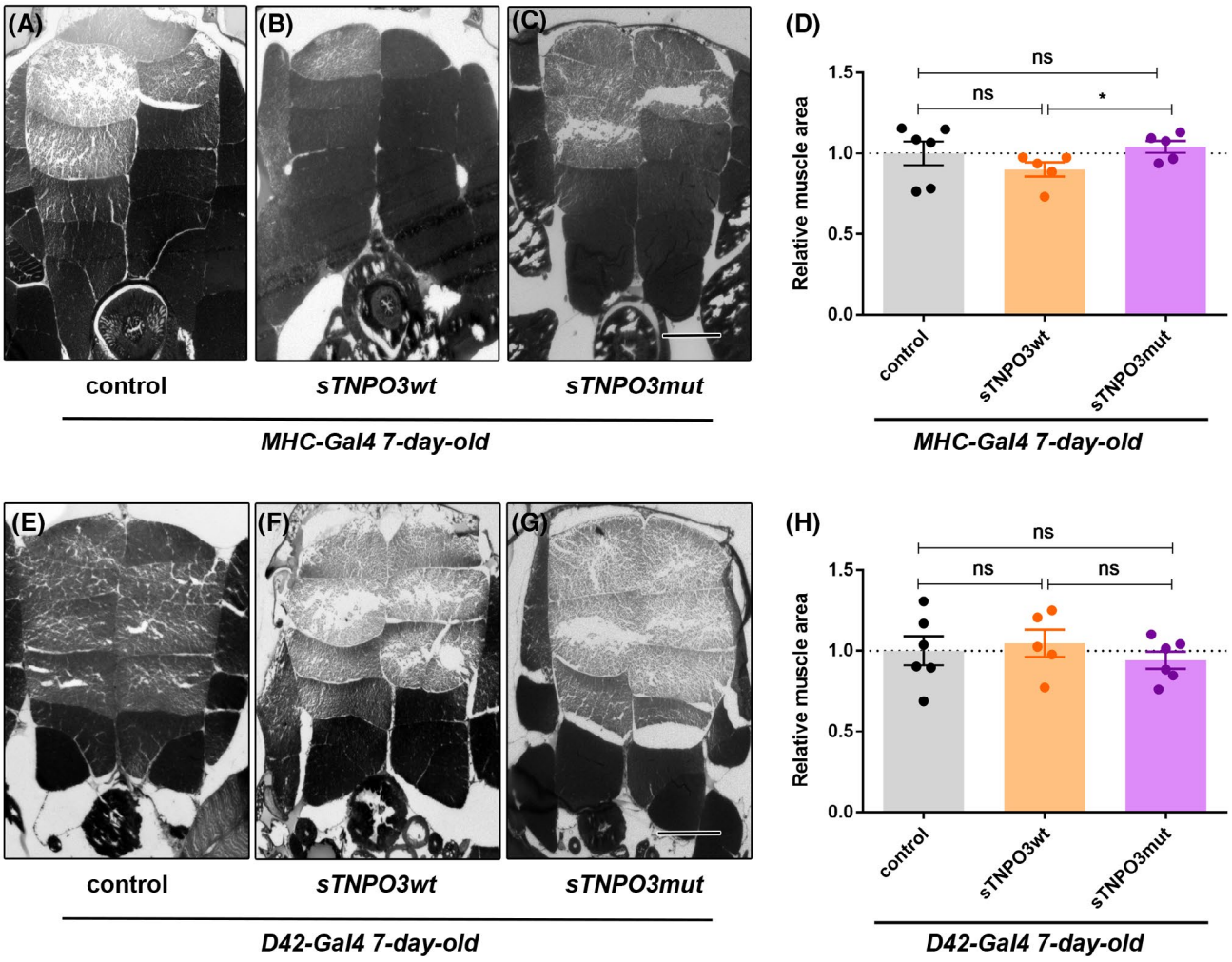

FIGURE 2 Expression of mutant *TNPO3* on a sensitized background does not generate muscle atrophy in IFM in 7-day-old flies. Representative dorsoventral sections of resin-embedded thoraces of 7-day-old flies expressing the indicated transgenes under the control of *MHC-Gal4* (A–C) or *D42-Gal4* (E–G) drivers. Relative muscle area was analyzed in control (gray bars; *MHC* or *D42-Gal4>UAS-GFP*), *sTNPO3wt* (orange bars; *MHC* or *D42-Gal4>UAS-TNPO3wt; UAS-IR-Tnpo-SR*), and *sTNPO3mut* flies (purple bars; *MHC* or *D42 -Gal4>UAS-TNPO3mut; UAS-IR-Tnpo-SR*). (D, H) Relative quantification of the mean percentage of muscle area per condition ($n = 6$). Scatter plots represent the means ± SEM. *$p < .05$, according to Student's *t*-test. Scale bar, 100 μm

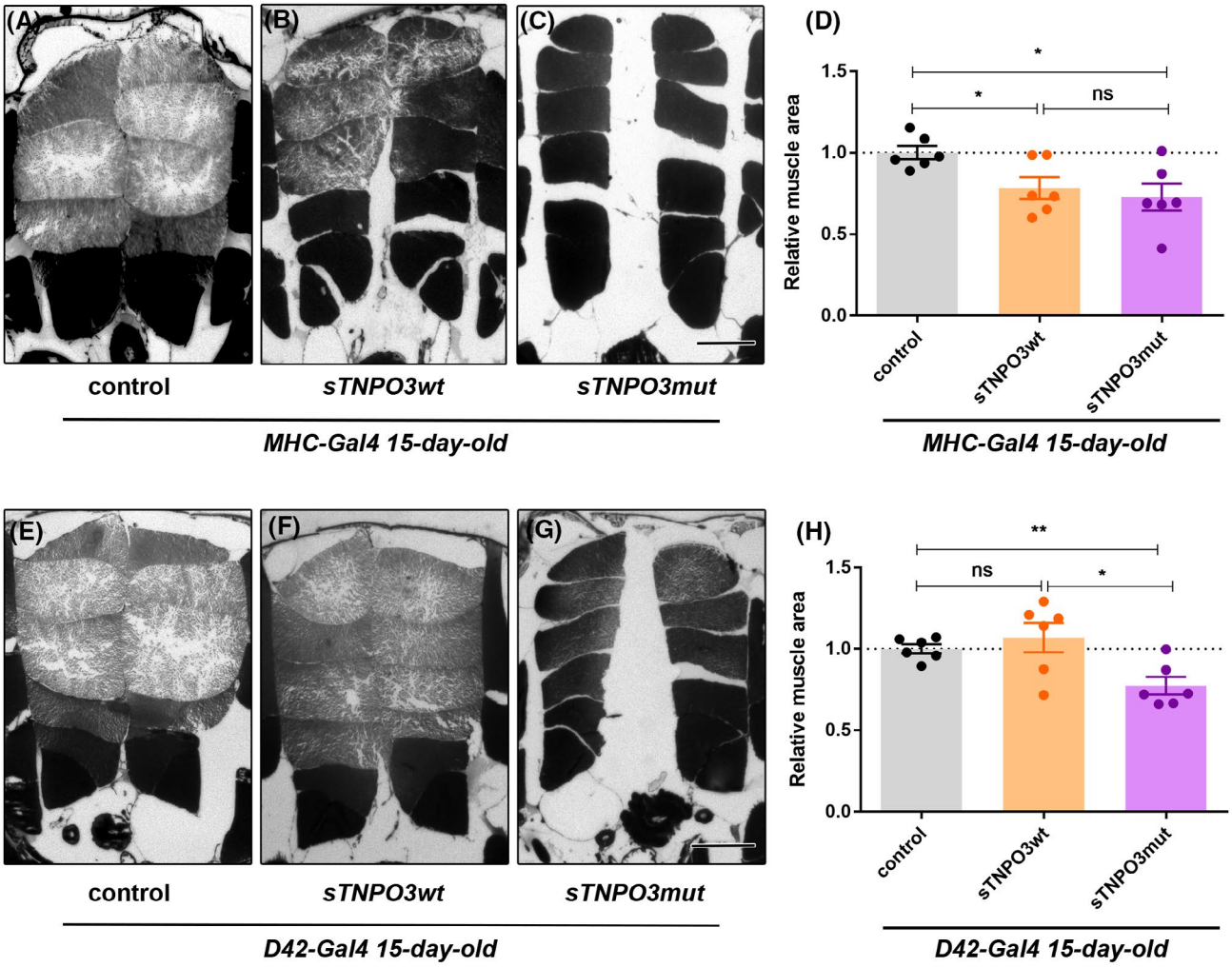

FIGURE 3 15-day-old LGMDD2 model fly display reduced IFM area. (A–C, E–G) Representative dorsoventral sections of resin-embedded thoraces of 15-day-old from control (gray bars; *MHC* or *D42-Gal4>UAS-GFP*), *sTNPO3wt* (orange bars; *MHC* or *D42-Gal4>UAS-TNPO3wt; UAS-IR-Tnpo-SR*), and *sTNPO3mut* flies (purple bars; *MHC* or *D42-Gal4>UAS-TNPO3mut; UAS-IR-Tnpo-SR*). (D, H) Relative quantification of the mean percentage of muscle area per condition ($n = 6$). Scatter plots represent the means ± SEM. $*p < .05$, $**p < .01$ according to Student's *t*-test. Scale bar, 100 μm

phenotype of IFM needs at least 15 days to develop, indicating that *TNPO3mut* expression on a *Tnpo-SR*-silenced background enhances atrophic phenotype over time, thus leading to muscle degeneration as the phenotype worsens with the individuals' age. Furthermore, these data indicate that *TNPO3mut* expression in motor neurons induces non-autonomous fly muscle degeneration, and its absence when *TNPO3wt* is expressed in motor neurons shows that this effect is specific to the LGMDD2 mutation.

To test whether the LGMDD2 mutation in *TNPO3* induced similar phenotypes in different *Drosophila* muscle types, we analyzed the morphology of the abdominal muscles running parallel to the dorsal vessel. Within the somatic musculature of the adult fly, abdominal muscles are tubular, with laterally aligned sarcomeres and synchronous contraction, in contrast to IFM, which are fibrillar muscles.[47] Specifically, we analyzed the abdominal segments A4 as, after dissection, these fibers remained exposed and intact. Thus, enabling the acquisition of better micrographs under the microscope useful for accurately measure their diameter. Moreover, we have chosen abdominal segments that were closest to the heart as they were the longest. Thus, we could perform three different measurements at distant points in each segment.

In muscle-specific expression, 15-day-old *sTNPO3mut* flies showed significantly thinner A4 muscle fibers than control (27%; *MHC-Gal4>UAS-GFP*) or *sTNPO3wt* flies (22% thinner) (Figure 4A–D). Turning to expression in motor neurons, there was also a significant reduction in A4 fiber width of *sTNPO3mut* flies compared to control flies (23% thinner; *D42-Gal4>UAS-GFP*) (Figure 4E–H). In contrast to IFM,

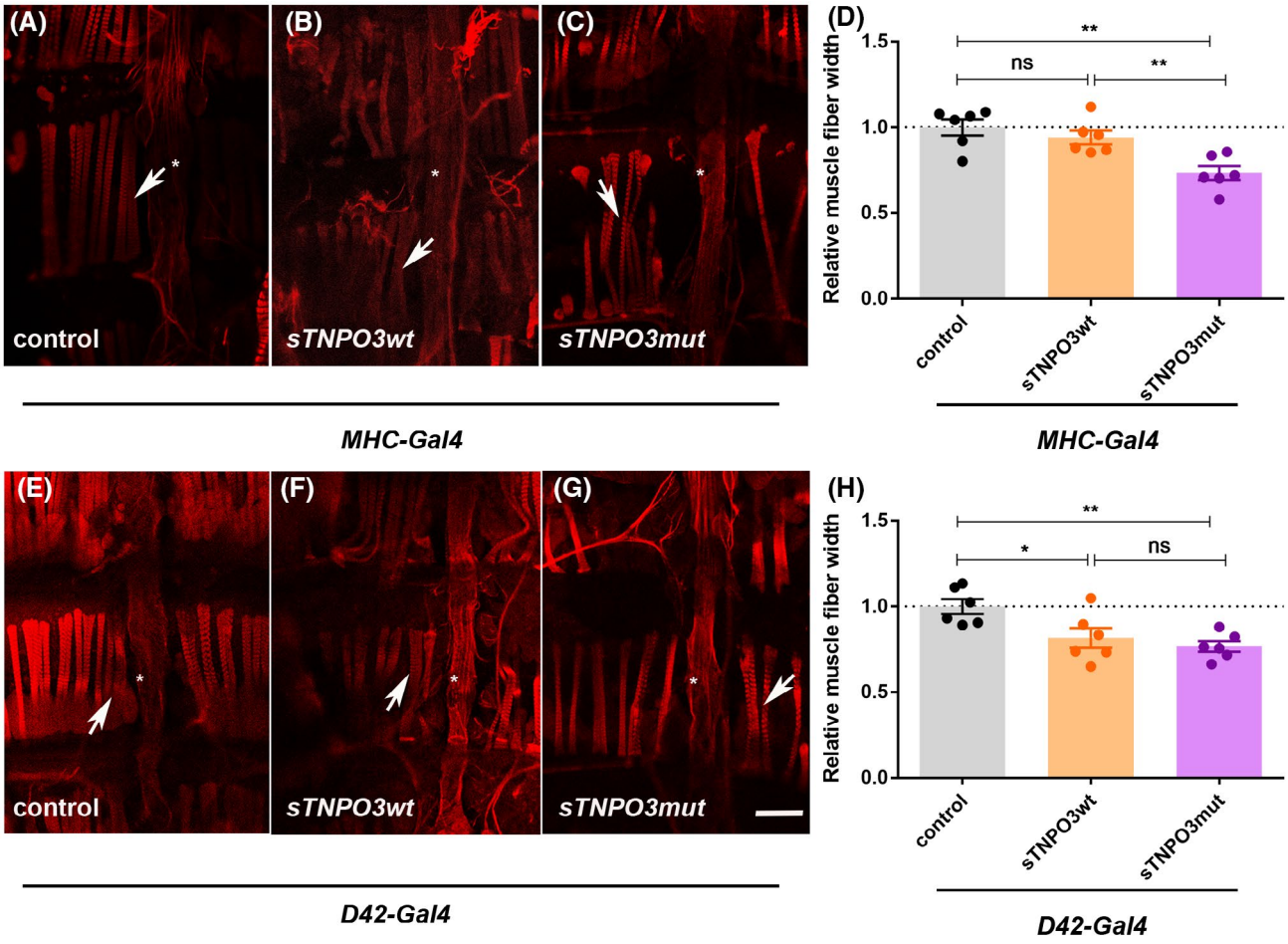

FIGURE 4 Atrophic phenotype in the abdominal muscles of LGMDD2 model flies. (A–C, E–G) Representative confocal images of rostral-caudal sections of the abdomen of 15-day-old flies stained with phalloidin (red). Transgene expression was under the control of *MHC-Gal4* or *D42-Gal4* drivers. The width of abdominal muscle fiber A4 was measured in control (gray bars; *MHC* or *D42-Gal4>UAS-GFP*), *sTNPO3wt* (orange bars; *MHC* or *D42-Gal4>UAS-TNPO3wt; UAS-IR-Tnpo-SR*), and *sTNPO3mut* (purple bars; *MHC* or *D42 -Gal4>UAS-TNPO3mut; UAS-IR-Tnpo-SR*) flies. (D, H) Thickness quantification of the indicated abdominal muscles in each condition relative to controls ($n = 6$). Asterisks mark the fly heart and arrows mark representative A4 fibers. Scatter plots represent the means ± SEM. *$p < .05$, **$p < .01$ according to Student's *t*-test. Scale bar, 50 μm

however, flies expressing *TNPO3wt* in motor neurons also had significantly thinner A4 fibers (18%), showing a phenotype like muscle-specific expression. Taken together, targeted expression of *TNPO3mut* in fly muscles and motor neurons reproduced the muscle atrophy of LGMDD2 patients in both IFM and abdominal muscles of 15-day-old flies, but while IFM were refractory to muscle degeneration upon *TNPO3wt* overexpression in motor neurons, abdominal muscles showed a similar response.

3.3 | LGMDD2 model flies show reduced locomotor activity

To assess the functional consequences of muscle degeneration detected upon *TNPO3mut* expression in muscles or motor neurons, we quantified climbing and flight ability in 7- and 15-day-old flies. For muscle-specific expression, climbing capacity decreased similarly for *sTNPO3mut* flies at both ages (64% and 63%, respectively) (Figure 5A,B) compared to control flies (*yw; MHC-Gal4*) and compared to *sTNPO3wt* flies at 15-day-old (54% reduction). However, *sTNPO3wt* fly climbing ability was reduced compared to controls only at 7 but not at 15 days old. In terms of flight, *TNPO3mut* expression in muscle reduced the average landing height in 15-day-old flies compared to control flies (15% reduction; *MHC-Gal4>UAS-GFP*) (Figure 5C), but differences in landing distance were not significantly different between *sTNPO3wt* and *sTNPO3mut* flies. This indicates that *TNPO3mut* expression in *Drosophila* muscles reduces locomotor activity of flies over time.

TNPO3mut expression in motor neurons also decreased climbing capacity in 7- and 15-day-old flies

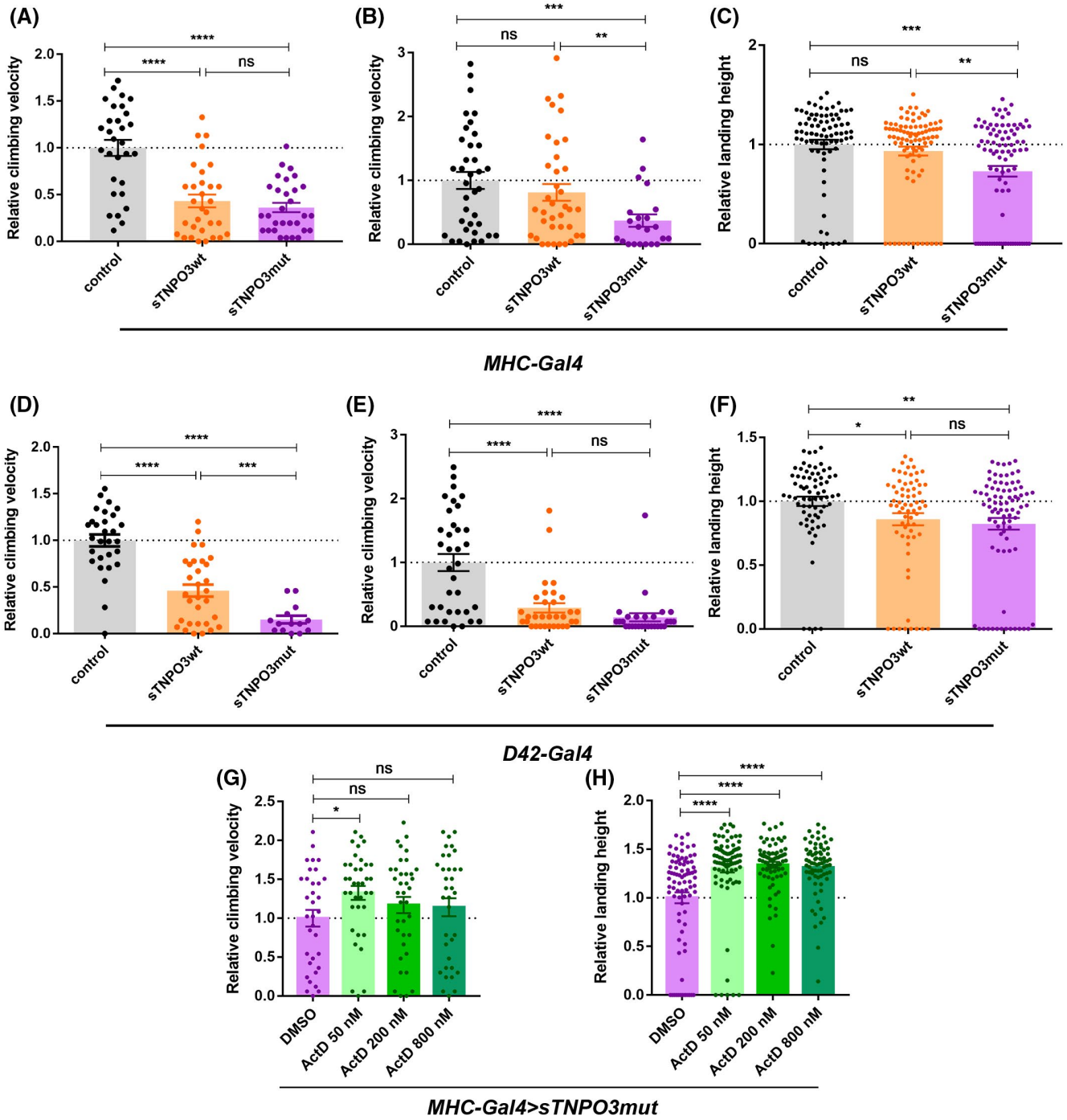

FIGURE 5 Locomotion activity is impaired in LGMDD2 model flies. *TNPO3* transgenes were co-expressed with an RNAi construct against the endogenous *Tnpo-SR* transcripts in the somatic musculature under the control of the *MHC-Gal4* driver or in the motor neurons with the *D42-Gal4* driver. Climbing velocity is represented relative to controls ± SEM. (80 < n < 100) of control (gray bars; *yw; MHC* or *D42-Gal4>UAS-GFP*), *sTNPO3wt* (orange bars; *MHC* or *D42-Gal4>UAS-TNPO3wt; UAS-IR-Tnpo-SR*), and *sTNPO3mut* flies (purple bars; *MHC* or *D42 -Gal4>UAS-TNPO3mut; UAS-IR-Tnpo-SR*) of 7 or 15 days old, expressing transgenes with the indicated drivers (A, B, D, E). (C, F) Graphs of flight assays represent the relative landing distance reached by the different experimental groups (80 < *n* < 100). The scatter plot represents the relative landing height ± SEM. The experiments were performed using 7 (A, D) and 15-day-old flies (B, C, E, F). *MHC/D42-Gal4>UAS-GFP* was considered as control flies. **p* < .05; ***p* < .01; ****p* < .001; *****p* < .0001 (Student's *t*-test). (G, H) Locomotor capacity was recovered after treating flies *sTNPO3mut* under the *MHC-Gal4* driver with 50, 200, or 800 nM ActD or with 0.1% DMSO as vehicle for 15 days. All data were normalized to values obtained in the corresponding control cohort. The scatter plot represents the relative climbing velocity and landing height ± SEM. **p* < .05; *****p* < .0001 according to one-way ANOVA test

compared to control flies (85% and 86%, respectively; *yw; D42-Gal4*) (Figure 5D,E). *TNPO3wt* expression in motor neurons also significantly reduced climbing velocity at 7- and 15-day-old, but comparing the effect of *TNPO3mut* vs. *TNPO3wt* there was a further reduction in climbing velocity at 7- and 15-day-old (44% and 54%, respectively). Regarding the flight capacity, *TNPO3mut* expression in fly motor neurons significantly reduced average landing height compared to the control flies (18% reduction; *D42-Gal4>UAS-GFP*), like the effect of *TNPO3wt* overexpression (Figure 5F). Ergo, *TNPO3mut* expression in *Drosophila* motor neurons also reduces locomotor activity of flies over time. Taking these data together, we conclude that the LGMDD2 fly model reproduces the impaired muscle function typical of LGMDD2 patients as demonstrated with *Drosophila* climbing and flight assays. Moreover, our data demonstrate that the lack of muscle function in the fly induced by TNPO3mut occurs over time, and after 7 days of age, loss of function may be related to the previously observed muscle degeneration.

Additionally, we studied functional phenotypes in LGMDD2 model fly treated with ActD and we observed a significant improvement of climbing and flight ability in treated flies, indicating that TNPO3mut has a toxic effect (Figure 5G,H).

3.4 | TNPO3mut reduces median survival and fly' eclosion capacity in *Drosophila*

To study whether *TNPO3mut* expression on a sensitized background had any effect on fly eclosion, we obtained their survival curves and quantified the percentage of emerged adults. The survival of flies expressing *TNPO3mut* in muscle compared to *sTNPO3wt* and control flies (*MHC-Gal4>UAS-IR-bcd*) fell dramatically until around day 28 when model flies approached controls. This led to significantly shorter median survival for TNPO3mut flies (25 days) than TNPO3wt and control flies (29 days) but the same maximal life expectancy for all three genotypes (Figure 6A,B). Regarding *TNPO3mut* expression in motor neurons, there was a significant reduction in the survival of *sTNPO3mut* flies against control flies (*D42-Gal4>UAS-IR-bcd*). The half-life of the different genotypes differed significantly, with 30 days for control, 26 days for *sTNPO3wt*, and 25 days for *sTNPO-3*mut flies (Figure 6E,F). Consequently, *TNPO3mut* expression in muscle or motor neurons in a genetically sensitized background significantly worsened survival of LGMDD2 model flies.

We also studied whether *TNPO3mut* or *TNPO3wt* expression affected fly development, by quantifying the percentage of individuals reaching pupa and adult stage. Generally, flies expressing either construct in both muscle and motor neurons reached pupation normally, without significant differences (Figure S4). In terms of adult eclosion capacity, *TNPO3mut* expression in fly muscle did not significantly reduce the percentage of adult flies compared to *sTNPO3wt* and control flies *(MHC-Gal4>UAS-GFP*) (Figure 6C). However, from day 7 onwards, a proportion of flies expressing *TNPO3mut* in the muscle developed a characteristic upheld wing phenotype (Figure 6D). *TNPO3mut* expression in motor neurons, in contrast, did cause a significant decrease eclosion of 57% and 58% compared to *sTNPO3wt* and control flies (*D42-Gal4>UAS-GFP*) (Figure 6G), respectively. Indeed, in these *sTNPO3mut* flies, we observed several examples of death at pharate stage half inside the pupae, compared to control lines in which development was complete and the pupae empty. In addition, a high proportion of flies expressing *TNPO3mut* in motor neurons had a wrinkled wing phenotype (Figure 6H). Therefore, specifically TNPO3mut reduces the emerging capacity of flies when expressed in motor neurons, also affecting fly wing development.

3.5 | Autophagy is upregulated in LGMDD2 model flies and an autophagy blocker, CQ, rescues TNPO3mut muscle phenotypes

Autophagy has been reported as increased in LGMDD2 muscle biopsies.[8] We assessed expression levels of some relevant genes involved in different steps of autophagosome formation[48] and we observed significantly upregulated expression of *Atg4, Atg8a,* and *Atg12* in the LGMDD2 model flies when compared to *sTNPO3wt* expressing transgenes under the control of the *MHC-Gal4* driver, while *Atg7* and *Atg9* remained unchanged (Figure 7A).

The conjugation of *Atg8* with phosphatidylethanolamine and its deconjugation by *Atg4* is a very important step for isolation, elongation and/or complete closure of the membrane during the autophagosome formation. *Atg8* is present on both in the inner and outer membranes of these structures. *Atg12*, is present in the outer membrane and also participates in the conjugation of *Atg8* with phosphatidylethanolamine and is essential in the process of elongation and isolation of the membrane.[48]

To further characterize whether *TNPO3mut* expression interferes with the multi-step autophagy process, we used a GFP-tagged Atg8a transgene and expressed it

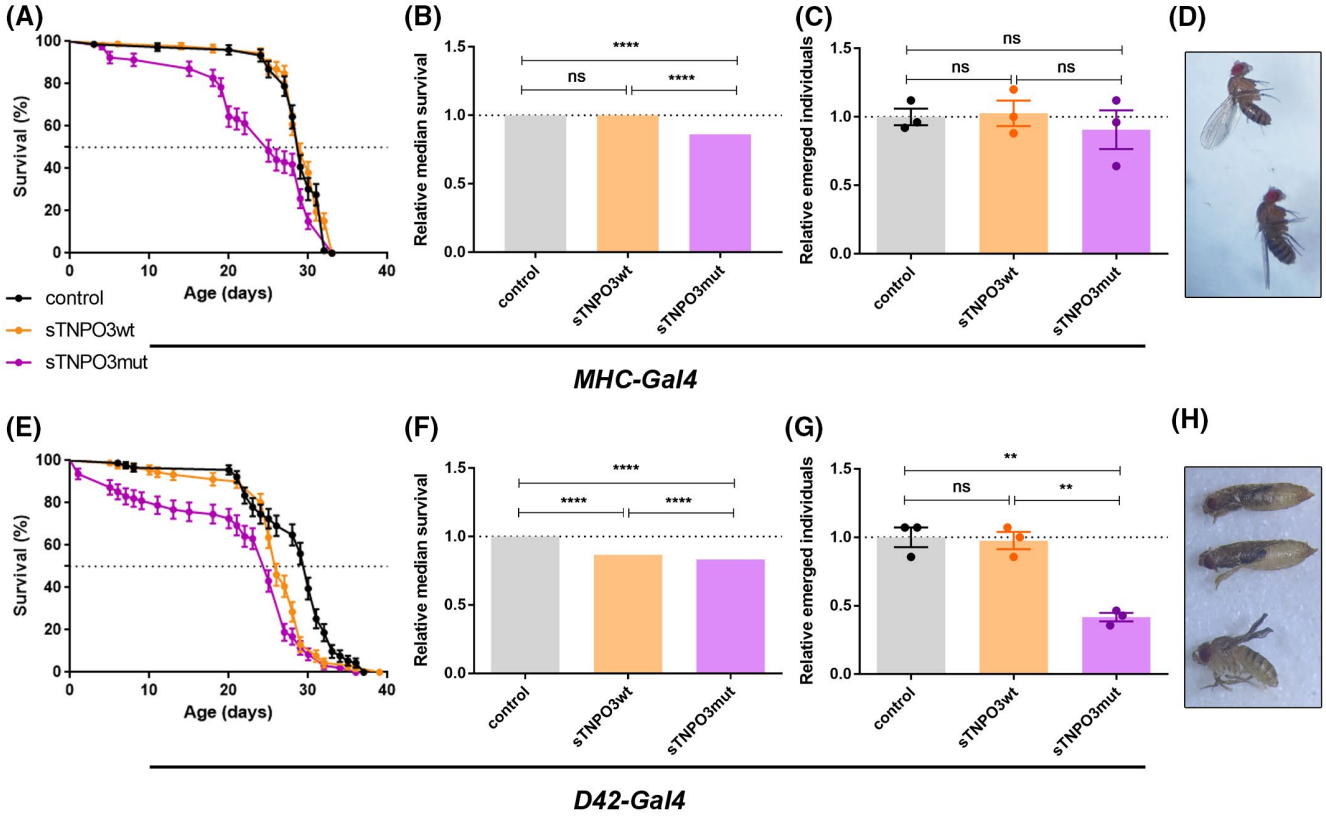

FIGURE 6 LGMDD2 model flies display defects in survival and eclosion phenotypes. (A, E) Survival curves and relative median survival (B, F) of control (gray, *UAS-IR-bcd*), *sTNPO3wt* (orange, *UAS-TNPO3wt; UAS-IR-Tnpo-SR*), and *sTNPO3mut* (purple, *UAS-TNPO3mut; UAS-IR-Tnpo-SR*) flies under the control of *MHC-Gal4* (A, B) or *D42-Gal4* (D, E) drivers. The survival curves are represented as a percentage of alive flies ($75 < n < 100$). (C, G) Analysis of the relative emerged individuals of the indicated conditions upon expression of transgenes in somatic muscle (C) or motor neurons (G) ($n = 75$). In all cases, the scatter plots represent the mean ± SEM of the indicated condition. $^{**}p < .01$; $^{****}p < .0001$ according to Student's *t*-test. (D, H) Representative images of adult flies of genotype *MHC/D42-Gal4>UAS-TNPO3mut; UAS-IR-Tnpo-SR*, respectively. Model flies expressing the transgene in the somatic musculature show upheld-wings phenotype (D) while the expression of the transgene in motor-neurons leads to flies unable to emerge from pupae and adult individuals with wrinkled wings (H)

concomitantly with *TNPO3wt* or *TNPO3mut* constructs under the control of the *MHC-Gal4* driver on a sensitized background. The *GFP:Atg8a* reporter is a widely used tool for monitoring autophagic degradation (or autophagic flux) in *Drosophila*.[26,49,50] In autolysosomes, lysosomal hydrolases will only degrade Atg8a, while free GFP remains in the cells due to its globular and compact structure. Accordingly, GFP can be visualized by fluorescence microscopy, and, autophagy induction can be quantified based on the appearance of puncta.[51] However, monitoring GFP:Atg8a does not determine flux unless used in conjunction with inhibitors of lysosomal fusion and/or degradation.[33] Chloroquine (CQ) is a well-characterized autophagy blocker, so we tested its effect on LGMDD2 flies (*MHC-Gal4 UAS-TNPO3mut; UAS-GFP:Atg8a UAS-IR-Tnpo-SR*), hereafter referred as sTNPO3mut; GFP:Atg8a. One-day-old adult *sTNPO3mut; GFP:Atg8a* flies were transferred to tubes containing standard medium supplemented with 10 or 100 μM CQ for 15 days and were compared to untreated *sTNPO3mut; GFP:Atg8a* flies (H_2O); as an additional control, we used *MHC-Gal4 UAS-TNPO3wt; UAS-GFP:Atg8a UAS-IR-Tnpo-SR* flies, hereafter referred as *sTNPO3wt; GFP:Atg8a*. Untreated *sTNPO3mut; GFP:Atg8a* flies showed a higher fluorescent signal than *sTNPO3wt; GFP:Atg8a* flies indicating an abnormal increase in autophagy in *Drosophila* muscles expressing *TNPO3mut* (Figure 7B–D). *sTNPO3mut; GFP:Atg8a* flies treated with 10 μM CQ reduced fluorescent signal slightly compared to untreated flies, but 100 μM CQ notably reduced the signal (Figure 7D–F).

In addition to a direct qualitative evaluation by fluorescence microscopy, we also quantified free GFP levels by western blot. This analysis showed a higher amount of GFP in *sTNPO3mut; GFP:Atg8a* flies compared to *sTNPO3wt; GFP:Atg8a*, which was significantly reduced upon 100 μM CQ (Figure 7G). These data confirm that

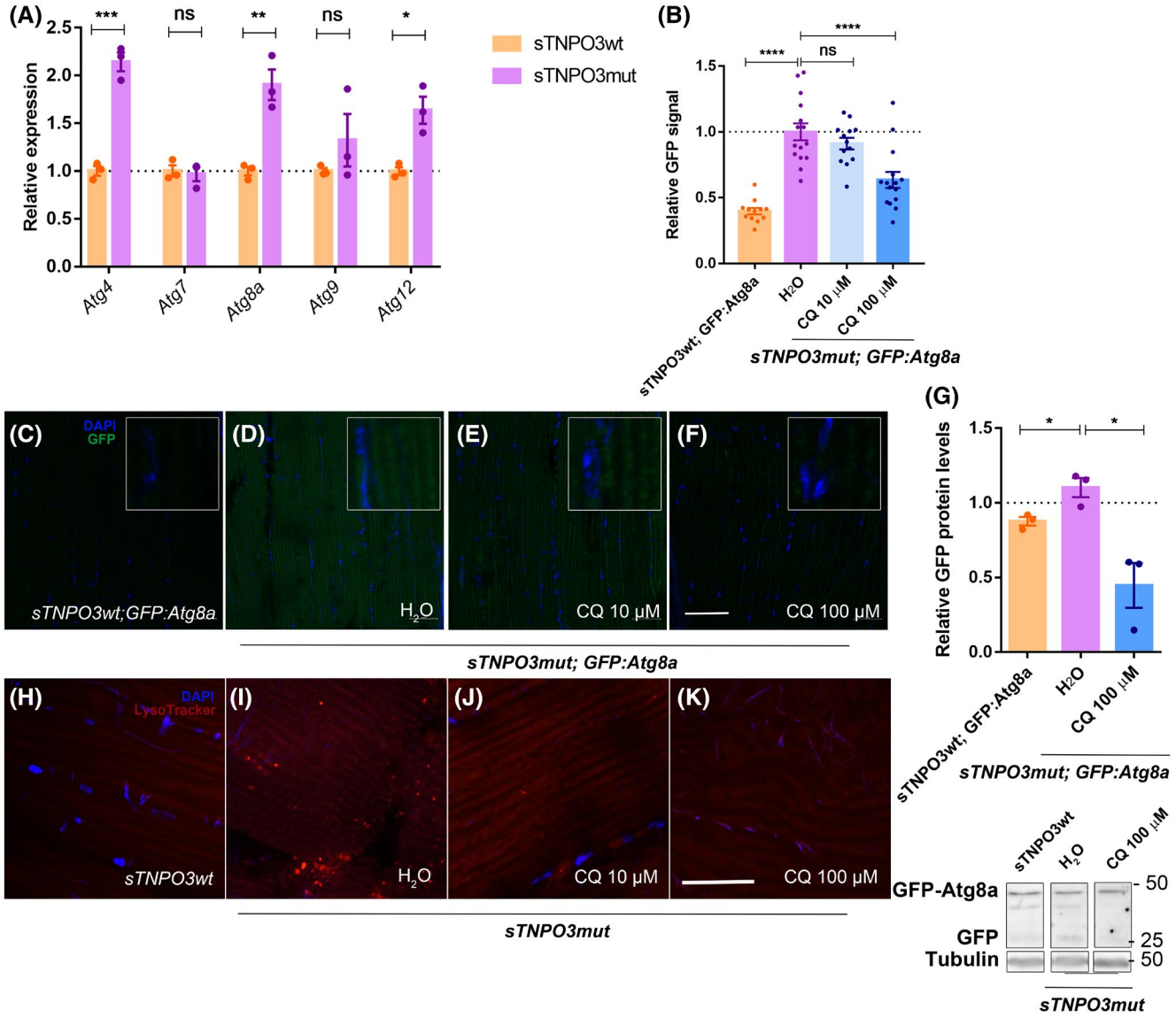

FIGURE 7 Autophagic flux is upregulated in LGMDD2 model flies with a sensitized background. Autophagy marker genes are upregulated in LGMDD2 flies with a sensitized background expressing *TNPO3mut* under the *MHC-Gal4* driver. Expression levels of *Atg4, Atg8a,* and *Atg12* were significantly increased (A). Expression was normalized to *Rp49* ($n = 3$). (B) Relative quantification of GFP signal from images of the conditions in C–F ($n = 4$). (C–F) Fluorescent confocal images of immunodetection of the GFP reporter (green) in IFM from transgenic fly lines expressing GFP:Atg8a show strong punctate staining in LGMDD2 model flies (*MHC-Gal4 UAS-TNPO3mut; UAS-GFP:Atg8a UAS-IR-Tnpo-SR*, D) compared to counterpart controls (*MHC-Gal4 UAS-TNPO3wt; UAS-GFP:Atg8a UAS-IR-Tnpo-SR,* C), indicating increased autophagic activity in model flies. The GFP signal became weaker in model flies treated with the indicated concentrations of CQ (E, F). Nuclei were counterstained with DAPI. Scale bar 20 μm. (G) Quantification and representative blots of protein extracts of flies with the genotypes and conditions in C, D, and F with the indicated antibodies ($n = 3$). Tubulin expression was used as an endogenous control. Fluorescent confocal images of LysoTracker staining (red) indicate increased puncta formation in model flies (I) compared to controls (H). A mild effect on the LysoTracker signal was observed when model flies were fed with 10 μM CQ (J), however, a strong reduction was detected after treatment with 100 μM CQ (K). Nuclei were counterstained with DAPI. Scale bar 40 μm. The scatter plot represents the means ± SEM. *$p < .05$; **$p < .01$; ***$p < .001$; ****$p < .0001$ according to Student's *t*-test

autophagy is significantly upregulated in LGMDD2 model flies with a sensitized background and that autophagy inhibition by CQ restored normal autophagic flux.

To further confirm increased autophagic flux in LGMDD2 model flies, we performed a LysoTracker staining in control flies (*MHC-Gal4 UAS-TNPO3wt; UAS-IR-Tnpo-SR*) and in *sTNPO3mut* flies (*MHC-Gal4 UAS-TNPO3mut; UAS-IR-Tnpo-SR*). LysoTracker is fluorophore with high selectivity for acidic organelles and consequently a dye to detect digesting autolysosomes.[33] We

observed strong signal in *sTNPO3mut* flies with marked bright dots spread over the surface of the thorax muscles (Figure 7I). These puncta, were not observed in control flies (Figure 7H). Upon CQ treatment of model flies dotted red signal disappeared recovering a control-like pattern of the staining (Figure 7J,K).

Since excessive catabolism by autophagic degradation can explain muscle atrophy in LGMDD2 patients, we studied the effect of CQ treatment on muscle atrophy in model flies. We first measured the IFM area of untreated *sTNPO3mut* flies and flies given 10 or 100 μM CQ in the nutritive medium (Figure 8A–D). Whereas no effect over the IFM cross-sectional muscle area was detected in *sTNPO3mut* flies after exposure to 10 μM CQ, sections of model flies treated with 100 μM CQ showed a significantly increased IFM area that reached 44% of untreated flies (Figure 8E). CQ oral administration to adult *sTNPO3mut* flies managed to rescue the muscle area, clearly indicating a muscle homeostasis contribution to the atrophic phenotype. To determine whether increased muscle area correlated with improved functional locomotion, we studied flying ability (Figure 8F). *sTNPO3mut* flies treated with 100 μM CQ increased their flight capacity by 47%, compared with untreated model flies. Considering that model flies showed impaired survival phenotype, we studied the effect of administering CQ throughout the adult life in *sTNPO3mut* flies (Figure 8G). While no impact on the longevity of treated individuals was detected, a clear beneficial effect on the mean life of model flies was dose-dependently observed. Specifically, *sTNPO3mut* flies showed a mean life of 29 days that was extended by 4 and 7 days after treatment with 10 and 100 μM CQ, respectively.

Besides, the wings of these flies were monitored daily, and a reduction in the upheld wing phenotype was detected in flies treated with 100 μM CQ (Figure 8H). Collectively, these observations confirm that the autophagy blocker CQ reverts atrophic phenotype and rescues muscle function of model flies. Remarkably, these results

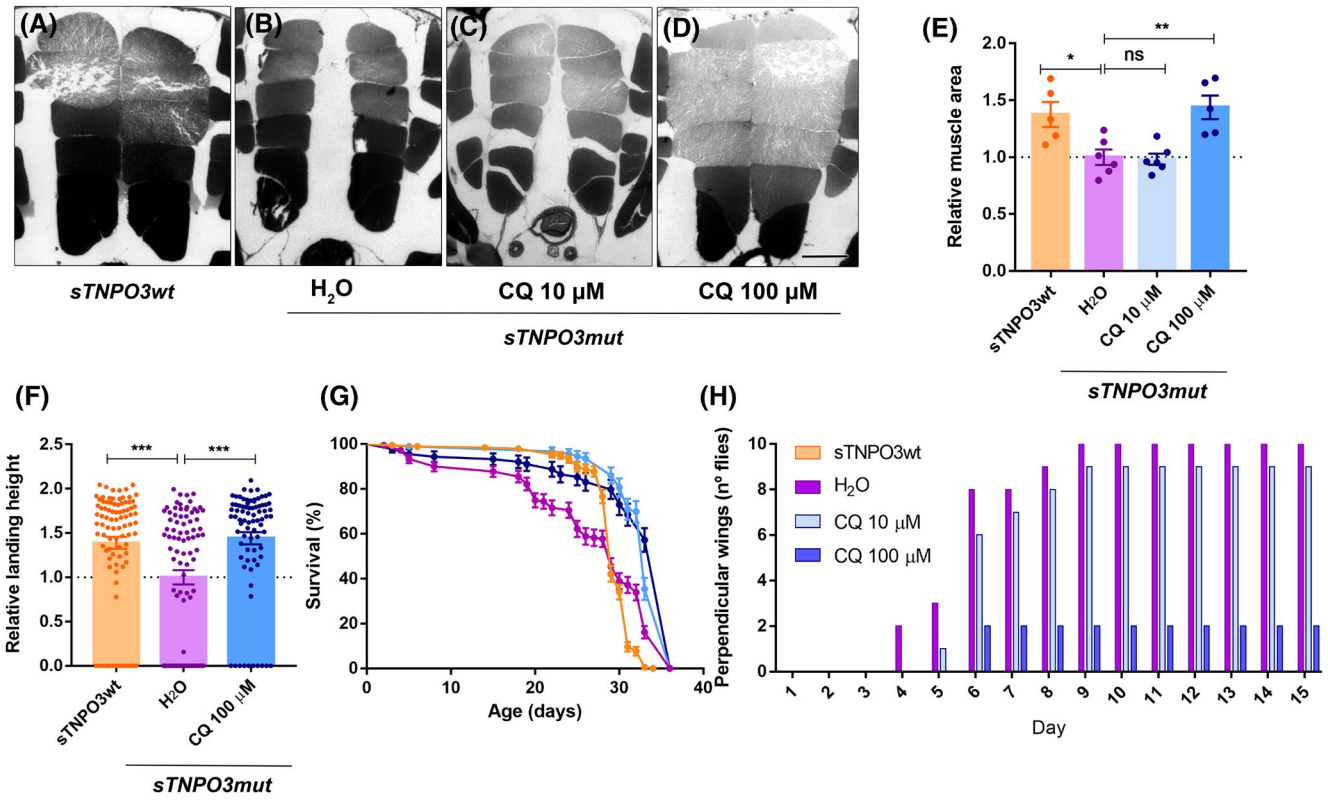

FIGURE 8 LGMDD2-related phenotypes are improved upon autophagy inhibition with CQ. (A–D) Dorsoventral sections of resin-embedded thoraces of control (*MHC-Gal4>UAS-TNPO3wt; UAS-IR-Tnpo-SR*) and LGMDD2 model flies (*MHC-Gal4>UAS-TNPO3mut; UAS-IR-Tnpo-SR*) treated with vehicle (H_2O) or CQ at the indicated concentrations (scale bar, 100 μm). (E) Relative quantification of the mean percentage of muscle area per condition ($n = 6$). (F) Plot of flight assays that represents the relative landing distance reached by *sTNPO3wt* flies or LGMDD2 model flies treated with vehicle (H_2O) or 100 μM CQ ($80 < n < 100$ in both cases). (G) Survival curves of the same experimental conditions as those described in F ($n = 100$). (H) Analysis of the percentage of model flies treated with vehicle (H_2O), 10 or 100 μM CQ with the upheld wing phenotype at the indicated time points ($n = 100$). The scatter plot represents the means ± SEM. $^*p < .05$; $^{**}p < .01$; $^{***}p < .001$ according to one-way ANOVA test

also demonstrate that LGMDD2 phenotypes in our model flies are reversible.

4 | DISCUSSION

LGMDD2 is an ultra-rare myopathy characterized by progressive proximal muscle weakness and atrophy primarily affecting pelvic limb muscles.[4,6] First identified in an Italo-Spanish family, it is caused by deletion of an adenine in the stop codon of the *TNPO3* gene which extends the C-terminal of the protein by 15 amino acids.[9,10] Although two new families and a sporadic case of LGMDD2 with different *TNPO3* mutations have recently been identified, 14 of the 15 amino acids initially described in the disease are conserved,[10–14] thus strongly supporting the pathogenic role of this sequence. Given that our *sTNPO-3mut* flies include this pathogenic sequence, we believe that our fly model will have general application to understand LGMDD2 despite the different mutations that may originate the disease. Notably, this first animal model of LGMDD2 in *Drosophila* will enable researchers to test hypotheses concerning the pathogenic mechanisms of the disease, as well as systematic testing of candidate drugs in the search for potential therapies.

TNPO3 is a member of the importin-β family of the Ran-GTP-dependent nuclear import proteins. The C-terminal domain of TNPO3 is essential for binding and nuclear transport of its cellular cargoes.[16,52] Significantly, LGMDD2 patients carry a heterozygous mutation in *TNPO3* that extends the C-terminal of the protein by 15 extra amino acids. As the cargo-binding domain of TNPO3 maps to this part of the molecule, this function might be altered in the mutated protein.[9,10] Moreover, it has been proposed that TNPO3 multimerizes to carry out its nuclear import functions.[16] In LGMDD2, the *TNPO3* mutation has been suggested to exert a dominant-negative effect,[10] implying that besides its altered function, it may also interfere with normal multimerization of TNPO3wt, further blocking its normal function.[18,53] Data from the *Drosophila* model support the hypothesis of dominant-negative pathogenesis since targeted expression of *TNPO3mut* to *Drosophila* IFM was insufficient to trigger significant muscle atrophy even after 4 weeks at 29°C. However, when the same overexpression conditions were combined with partial silencing of the *Drosophila TNPO3* gene ortholog, *Tnpo-SR*, we detected clear muscle reduction in IFM and abdominal muscles, suggesting that human *TNPO3mut* may act through a dominant-negative mechanism. Thus, under normal Tnpo-SR levels TNPO3mut might not displace enough protein dimers for significant functional reduction, whereas artificially lowering endogenous levels enables this process to occur.

Flies expressing human *TNPO3mut* in a sensitized *Tnpo-SR* background are the first in vivo LGMDD2 experimental model reported to date that reproduced several molecular, histological and functional defects also found in patients. At the molecular level, we observed increased TNPO3 levels in LGMDD2 model fly, accordingly to a previously described phenotype in LGMDD2 patient biopsies.[13] Furthermore, ActD treatment reduced mRNA and protein levels of TNPO3, and rescued functional phenotypes in LGMDD2 model flies. Taken together, these results suggest that the LGMDD2 mutation promotes the accumulation of TNPO3 at the protein level, either by improving the stability of the protein by posttranscriptional modifications or by enhancing it its transcription and/or translation. Moreover, it can be stated that the accumulation of TNPO3 is toxic.

Continuing with LGMDD2-like phenotypes reproduced by model fly, *Drosophila* muscles, including IFM and abdominals, showed signs of muscle atrophy quantified as cross-sectional muscle area reduction or width reduction. Histopathological signs were also degenerative in 15-day-old, but not 7-day-old flies, also affecting locomotive ability and median survival of animals (Figure 9). Locomotion measurements, however, were influenced by non-muscle phenotypes such as upheld and deformed wings. Generally, LGMDD2 patients are born healthy and impaired motor function and muscle atrophy occurs several months or even years after birth.[4,7,10–14] Therefore, our data suggest that TNPO3mut induces progressive muscle weakness and degeneration in LGMDD2 flies, as in patients.

LGMDD2 is a degenerative muscle disorder, but patients also display nervous system-related symptoms such as dysphagia and dysarthria.[4,7,54] In other degenerative muscle disorders, such as spinal muscular atrophy and amyotrophic lateral sclerosis, loss of muscle innervation leads to progressive degeneration of muscle fibers, in addition to potential autonomous effects within the muscles themselves.[55] TNPO3mut has been described in muscle of LGMDD2 patients, based on its reported expression pattern in humans, a plausible hypothesis is that the mutant protein will also be expressed in the spinal cord,[56] thus affecting the innervation of the muscle and ultimately causing muscle degeneration. *Drosophila* has proved a useful model to investigate neuromuscular diseases since it enables us to study the individual effects of a genetic mutation exclusively expressed in muscles or in motor neurons, using the Gal4/UAS system. Fundamental mechanisms of neuromuscular function in flies are remarkably well conserved, in processes ranging from action potential generation and propagation in the neuron, to synaptic transmission at the neuromuscular junction to excitation-contraction coupling in the muscle.[23,25,55]

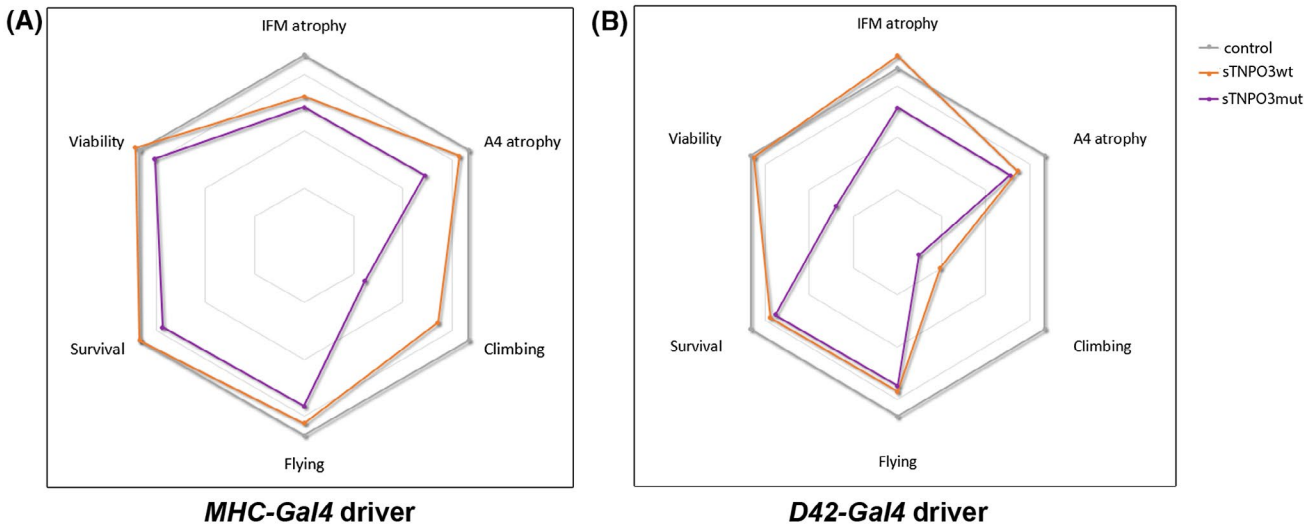

FIGURE 9 Radar chart representation of the six phenotypes analyzed in LGMDD2 model flies. Quantification of each phenotype was normalized to control values on a relative scale from 0 to 100 (normal), so that the external hexagon represents the normal parameters obtained using the *MHC-Gal4* (A) or with *D42-Gal4* driver (B). Note that while some parameters responded similarly to *sTNPO3wt* or *sTNPO3mut* (eg, IFM atrophy driven by *MHC-Gal4*), the response of others was strongly differential (eg, climbing capacity drive by *MHC-Gal4*). Overall, the greatest effects were observed for motor neurons-driven overexpression of *TNPO3mut*

In this study, we present the first LGMDD2 experimental model that can be used to verify the potential connection between TNPO3mut and loss of muscle innervation. As reported here, *TNPO3mut* expression in *Drosophila* motor neurons causes IFM and abdominal atrophy in 15-day-old flies, alters locomotor ability and reduces median survival (Figure 9). In addition, *TNPO3mut* expression in motor neurons dramatically reduced fly viability, and several TNPO3mut flies that were able to hatch had defective wing morphogenesis and died over the first days of life. Consequently, this study demonstrates the importance of TNPO3 for fly development and muscle preservation.

Although TNPO3 is a functional homolog of Tnpo-SR,[31] in our model significant differences between control and *sTNPO3wt* flies were observed in some assays. This may be because the expression of a copy of *TNPO3wt* triggers gain-of-function phenotypes and/or that the functional conservation between human and *Drosophila* proteins is not complete. Importantly, however, we found several examples where the phenotypes triggered by *TNPO3mut* or *TNPO3wt* were different (Figure 9), which distinguish pathogenic effects caused by the mutation itself from the overexpression phenotypes. Along these lines, although both *TNPO3wt* and *TNPO3mut* are inserted in the same genomic position in transgenic flies, molecular tests showed TNPO3mut transcripts and protein levels to be higher in the *Drosophila* model than in the wild type counterpart. Given the unlikelihood of effects at the transcription level, we favor the possibility that the extended open reading frame in the mutant transcripts may influence its stability[57] or that of the mutant protein.

Overactive autophagy has been reported in LGMDD2 biopsies,[8] and several studies have demonstrated that autophagy overactivation disrupts protein homeostasis in the muscle, and excessive catabolism ends up degrading and generates atrophy.[20,21] Indeed, in several muscular diseases characterized by muscle wasting, like Pompe disease or myotonic dystrophy type 1, autophagy is increased and its suppression shows beneficial effects in animal models of the disease.[26,41,58] To confirm whether TNPO3mut-induced autophagy was one of the molecular mechanisms responsible for muscle degeneration, on the one hand, we confirm the upregulation of Atg genes and increased autophagic flux in LGMDD2 model flies. And, on the other hand, we tested the effect of blocking this pathway by CQ treatment. Our data demonstrate that LGMDD2-like phenotypes were rescued at histological, functional, and molecular levels upon the CQ treatment. These findings are particularly interesting for two reasons: first, they confirm that overactivated autophagy leads to characteristic phenotypes of the disease, highlighting this route as a new therapeutic target to design disease treatments. Second, they confirm that the phenotypes generated by TNPO3mut are reversible. This is particularly encouraging in designing a therapeutic strategy, since in addition to avoiding the appearance of symptoms it opens the possibility of already developed disease phenotypes being reversed after treatment. Our data showed that drug inhibition of autophagy rescued

muscle atrophy in a model where *TNPO3mut* was continuously expressed in fly muscles. CQ also rescued upheld wings and flight phenotypes in model flies. Taken together, these data suggest that upregulated autophagy in LGMDD2 might be the cause of muscle degeneration in patients and pharmacological inhibition of autophagy by CQ is a valid strategy for improving phenotypes in model LGMDD2 flies. The ability to rescue muscle phenotypes and the reversibility of the atrophic phenotype observed in our LGMDD2 model provide proof of principle for therapeutic strategies aimed at limiting autophagy in adult muscles. Regulation of autophagy by CQ is not a novel proposal as a therapy for muscular dystrophies.[41] CQ is a potent autophagy inhibitor that works by blocking autophagosomes-lysosome fusion[32] yet safer alternatives that act at the same level in the autophagy pathway, such as hydroxychloroquine, are also currently accepted.[59]

In conclusion, in addition to reporting the first in vivo model of LGMDD2, by demonstrating TNPO3mut-induced muscle phenotypes in flies, this study has provided crucial insight into the mechanisms of LGMDD2 pathogenesis. First, we demonstrate a significant increase in mutant TNPO3 transcripts and protein, which could reveal specific post-transcriptional pathways triggered by the mutation which are potential targets for therapeutic intervention themselves. Second, we provide indirect evidence for a dominant-negative mechanism as the cause of LGMDD2 and proof of concept for the therapeutic relevance of modulating hyperactive autophagy in the disease model. Third, we propose that LGMDD2 may have a neurogenic component, based on the strong phenotypes detected in flies by expressing only human *TNPO3mut* in motor neurons. Finally, a robust rescue of muscle atrophy phenotypes was detected by treating adult flies exclusively with CQ, thus supporting the theory that TNPO3mut-induced muscle phenotypes are reversible, a pivotal finding in developing therapeutic strategies for LGMDD2 patients.

ACKNOWLEDGMENTS

This work was possible by funding from "Asociación Conquistando Escalones." The authors wish to thank Conquistando Escalones for their enormous effort in securing funding, their total confidence in our work and their extraordinary cooperation. A.B. and J.F.C. are grateful for the support of the Conselleria d'Educació, Investigació, Cultura i Esport (Generalidad Valenciana) as postdoctoral (APOSTD2017/077 and APOSTD2017/088) grantees. The equipment used in this research was partly funded by Generalitat Valenciana and co-financed with ERDF funds (OP ERDF of Comunitat Valenciana 2014–2020).

DISCLOSURES

The authors declare no competing interests.

AUTHORS' CONTRIBUTIONS

R.A. provided the conceptual framework for the study. R.A., A.B., A.B.B., and J.F.C. conceived and designed the experiments and helped interpretating the results. A.B.B., A.B., and J.F.C., performed the experiments and analyzed data A.B.B., A.B., and R.A. prepared the manuscript.

REFERENCES

1. Bushby K. Diagnosis and management of the limb girdle muscular dystrophies. *Pract Neurol*. 2009;9:314-323.
2. Nigro V, Savarese M. Genetic basis of limb-girdle muscular dystrophies: the 2014 update. *Acta Myol*. 2014;33:1-12.
3. Straub V, Murphy A, Udd B, et al. 229th ENMC international workshop: Limb girdle muscular dystrophies—nomenclature and reformed classification Naarden, the Netherlands, 17–19 March 2017. *Neuromuscul Disord*. 2018;28(8):702-710.
4. Gamez J, Navarro C, Andreu AL, et al. Autosomal dominant limb-girdle muscular dystrophy: a large kindred with evidence for anticipation. *Neurology*. 2001;56:450-454.
5. Palenzuela L, Andreu AL, Gàmez J, et al. A novel autosomal dominant limb-girdle muscular dystrophy (LGMD 1F) maps to 7q32.1-32.2. *Neurology*. 2003;61:404-406.
6. Fanin M, Peterle E, Fritegotto C, et al. Incomplete penetrance in limb-girdle muscular dystrophy type 1F. *Muscle Nerve*. 2015;52:305-306.
7. Peterle E, Fanin M, Semplicini C, Padilla JJV, Nigro V, Angelini C. Clinical phenotype, muscle MRI and muscle pathology of LGMD1F. *J Neurol*. 2013;260:2033-2041.
8. Cenacchi G, Peterle E, Fanin M, Papa V, Salaroli R, Angelini C. Ultrastructural changes in LGMD1F. *Neuropathology*. 2013;33:276-280.
9. Melià MJ, Kubota A, Ortolano S, et al. Limb-girdle muscular dystrophy 1F is caused by a microdeletion in the transportin 3 gene. *Brain*. 2013;136:1508-1517.
10. Torella A, Fanin M, Mutarelli M, et al. Next-generation sequencing identifies Transportin 3 as the causative gene for LGMD1F. *PLoS One*. 2013;8:1-7.
11. Gibertini S, Ruggieri A, Saredi S, et al. Long term follow-up and further molecular and histopathological studies in the LGMD1F sporadic TNPO3-mutated patient. *Acta Neuropathol Commun*. 2018;6:141.
12. Pál E, Zima J, Hadzsiev K, et al. A novel pathogenic variant in TNPO3 in a Hungarian family with limb-girdle muscular dystrophy 1F. *Eur J Med Genet*. 2019;62:103662.
13. Vihola A, Palmio J, Danielsson O, et al. Novel mutation in TNPO3 causes congenital limb-girdle myopathy with slow progression. *Neurol Genet*. 2019;5:1-9.
14. Angelini C, Marozzo R, Pinzan E, et al. A new family with transportinopathy: increased clinical heterogeneity. *Ther Adv Neurol Disord*. 2019;12:175628641985043.
15. Sapra AK, Änkö ML, Grishina I, et al. SR protein family members display diverse activities in the formation of nascent and mature mRNPs in vivo. *Mol Cell*. 2009;34:179-190.

16. Maertens GN, Cook NJ, Wang W, et al. Structural basis for nuclear import of splicing factors by human Transportin 3. *Proc Natl Acad Sci U S A*. 2014;111:2728-2733.
17. De Iaco A, Luban J. Inhibition of HIV-1 infection by TNPO3 depletion is determined by capsid and detectable after viral cDNA enters the nucleus. *Retrovirology*. 2011;8:98.
18. Rodríguez-Mora S, De Wit F, García-Perez J, et al. The mutation of Transportin 3 gene that causes limb girdle muscular dystrophy 1F induces protection against HIV-1 infection. *PLoS Pathog*. 2019;15:e1007958.
19. Costa R, Rodia MT, Zini N, et al. Morphological study of TNPO3 and SRSF1 interaction during myogenesis by combining confocal, structured illumination and electron microscopy analysis. *Mol Cell Biochem*. 2021;476:1797-1811.
20. Mammucari C, Milan G, Romanello V, et al. FoxO3 controls autophagy in skeletal muscle in vivo. *Cell Metab*. 2007;6:458-471.
21. Zhao J, Brault JJ, Schild A, et al. FoxO3 coordinately activates protein degradation by the autophagic/lysosomal and proteasomal pathways in atrophying muscle cells. *Cell Metab*. 2007;6:472-483.
22. Garcia-Lopez A, Monferrer L, Garcia-Alcover I, Vicente-Crespo M, Alvarez-Abril MC, Artero RD. Genetic and chemical modifiers of a CUG toxicity model in Drosophila. *PLoS One*. 2008;3(2):e1595.
23. Lloyd TE, Taylor JP. Flightless flies: *Drosophila* models of neuromuscular disease. *Ann N Y Acad Sci*. 2010;1184(1):E1-E20.
24. Fernandez-Costa JM, Garcia-Lopez A, Zuñiga S, et al. Expanded CTG repeats trigger miRNA alterations in *Drosophila* that are conserved in myotonic dystrophy type 1 patients. *Hum Mol Genet*. 2013;22:704-716.
25. Rai M, Nongthomba U, Grounds MD. Skeletal muscle degeneration and regeneration in mice and flies. In: *Current Topics in Developmental Biology*. Vol. 108. Academic Press Inc.; 2014:247-281.
26. Bargiela A, Cerro-Herreros E, Fernandez-Costa JM, Vilchez JJ, Llamusi B, Artero R. Increased autophagy and apoptosis contribute to muscle atrophy in a myotonic dystrophy type 1 *Drosophila* model. *DMM Dis Model Mech*. 2015;8:679-690.
27. Cerro-Herreros E, González-Martínez I, Moreno-Cervera N, et al. Therapeutic potential of AntagomiR-23b for treating myotonic dystrophy. *Mol Ther Nucleic Acids*. 2020;21:837-849.
28. Konieczny P, Artero R. *Drosophila* SMN2 minigene reporter model identifies moxifloxacin as a candidate therapy for SMA. *FASEB J*. 2020;34:3021-3036.
29. Allikian MJ, Bhabha G, Dospoy P, et al. Reduced life span with heart and muscle dysfunction in *Drosophila* sarcoglycan mutants. *Hum Mol Genet*. 2007;16:2933-2943.
30. Li S, Zhang P, Freibaum BD, et al. Genetic interaction of hnRNPA2B1 and DNAJB6 in a *Drosophila* model of multisystem proteinopathy. *Hum Mol Genet*. 2016;25:936-950.
31. Allemand E, Dokudovskaya S, Bordonné R, Tazi J. A conserved *Drosophila* transportin-serine/arginine-rich (SR) protein permits nuclear import of *Drosophila* SR protein splicing factors and their antagonist repressor splicing factor 1. *Mol Biol Cell*. 2002;13:2436-2447.
32. Mauthe M, Orhon I, Rocchi C, et al. Chloroquine inhibits autophagic flux by decreasing autophagosome-lysosome fusion. *Autophagy*. 2018;14:1435-1455.
33. Klionsky DJ, Abdel-Aziz AK, Abdelfatah S, et al. Guidelines for the use and interpretation of assays for monitoring autophagy. *Autophagy*. 2021;17:1-382.
34. Brand H, Perrimon N. Targeted gene expression as a means of altering cell fates and generating dominant phenotypes. *Development*. 1993;118(2):401-415.
35. Markstein M, Pitsouli C, Villalta C, Celniker SE, Perrimon N. Exploiting position effects and the gypsy retrovirus insulator to engineer precisely expressed transgenes. *Nat Genet*. 2008;40:476-483.
36. Livak KJ, Schmittgen TD. Analysis of relative gene expression data using real-time quantitative PCR and the 2-ΔΔCT method. *Methods*. 2001;25:402-408.
37. Schneider CA, Rasband WS, Eliceiri KW. NIH Image to ImageJ: 25 years of image analysis. *Nat Methods*. 2012;9:671-675.
38. Llamusi B, Bargiela A, Fernandez-Costa JM, et al. Muscleblind, BSF and TBPH are mislocalized in the muscle sarcomere of a *Drosophila* myotonic dystrophy model. *DMM Dis Model Mech*. 2013;6:184-196.
39. Selma-Soriano E, Llamusi B, Fernández-Costa JM, Ozimski LL, Artero R, Redón J. Rabphilin involvement in filtration and molecular uptake in *Drosophila* nephrocytes suggests a similar role in human podocytes. *DMM Dis Model Mech*. 2020:13.
40. Chakraborty M, Selma-Soriano E, Magny E, et al. Pentamidine rescues contractility and rhythmicity in a *Drosophila* model of myotonic dystrophy heart dysfunction. *Dis Model Mech*. 2015;12:1569-1578. https://doi.org/10.1242/dmm.021428
41. Bargiela A, Sabater-Arcis M, Espinosa-Espinosa J, Zulaica M, De Munain AL, Artero R. Increased Muscleblind levels by chloroquine treatment improve myotonic dystrophy type 1 phenotypes in in vitro and in vivo models. *Proc Natl Acad Sci U S A*. 2019;116:25203-25213.
42. Hunt LC, Demontis F. (2013) Whole-mount immunostaining of *Drosophila* skeletal muscle. *Nat Protoc*. 2013;812(8):2496-2501.
43. Babcock DT, Ganetzky B. An improved method for accurate and rapid measurement of flight performance in *Drosophila*. *J Vis Exp*. 2014;13:e51223.
44. Spring AM, Raimer AC, Hamilton CD, Schillinger MJ, Matera AG. Comprehensive modeling of spinal muscular atrophy in *Drosophila melanogaster*. *Front Mol Neurosci*. 2019;12.
45. Perkins LA, Holderbaum L, Tao R, et al. The transgenic RNAi project at Harvard medical school: resources and validation. *Genetics*. 2015;201:843-852.
46. Smith CE. Actinomycin binding to DNA: mechanism and specificity. *J Mol Biol*. 1965;11:445-457.
47. Dobi KC, Schulman VK, Baylies MK. Specification of the somatic musculature in *Drosophila*. *Wiley Interdiscip Rev Dev Biol*. 2015;4:357-375.
48. Mizushima N, Yoshimori T, Ohsumi Y. The role of Atg proteins in autophagosome formation. *Annu Rev Cell Dev Biol*. 2011;27(1):107–132. 10.1146/annurev-cellbio-092910-154005
49. Nagy P, Varga Á, Pircs K, Hegedus K, Juhász G. Myc-driven overgrowth requires unfolded protein response-mediated induction of autophagy and antioxidant responses in *Drosophila melanogaster*. *PLoS Genet*. 2013;9:e1003664.
50. Takáts S, Nagy P, Varga Á, et al. Autophagosomal Syntaxin17-dependent lysosomal degradation maintains neuronal function in *Drosophila*. *J Cell Biol*. 2013;201:531-539.

51. Mauvezin C, Ayala C, Braden CR, Kim J, Neufeld TP. Assays to monitor autophagy in *Drosophila*. *Methods*. 2014;68:134-139.
52. Lai MC, Lin RI, Tarn WY. Transportin-SR2 mediates nuclear import of phosphorylated SR proteins. *Proc Natl Acad Sci U S A*. 2001;98:10154-10159.
53. Costa R, Rodia MT, Vianello S, et al. Transportin 3 (TNPO3) and related proteins in limb girdle muscular dystrophy D2 muscle biopsies: a morphological study and pathogenetic hypothesis. *Neuromuscul Disord*. 2020;30:685-692.
54. Knuijt S, Kalf JG, De Swart BJM, et al. Dysarthria and dysphagia are highly prevalent among various types of neuromuscular diseases. *Disabil Rehabil*. 2014;36:1285-1289.
55. Kreipke RE, Kwon YV, Shcherbata HR, Ruohola-Baker H. *Drosophila melanogaster* as a model of muscle degeneration disorders. In: *Current Topics in Developmental Biology*. Vol. 121. Academic Press Inc.; 2017:83-109.
56. The GTEx Consortium. The GTEx Consortium atlas of genetic regulatory effects across human tissues. *Science*. 2020:369;1318-1330.
57. Mauger DM, Joseph Cabral B, Presnyak V, et al. mRNA structure regulates protein expression through changes in functional half-life. *Proc Natl Acad Sci U S A*. 2019;116:24075-24083.
58. Raben N, Hill V, Shea L, et al. Suppression of autophagy in skeletal muscle uncovers the accumulation of ubiquitinated proteins and their potential role in muscle damage in Pompe disease. *Hum Mol Genet*. 2008;17:3897-3908.
59. Tavakol S, Ashrafizadeh M, Deng S, et al. Autophagy modulators: mechanistic aspects and drug delivery systems. *Biomolecules*. 2019;9:530.

SUPPORTING INFORMATION

Additional Supporting Information may be found online in the Supporting Information section.

How to cite this article: Blázquez-Bernal Á, Fernandez-Costa JM, Bargiela A, Artero R. Inhibition of autophagy rescues muscle atrophy in a LGMDD2 *Drosophila* model. *FASEB J*. 2021;35:e21914. https://doi.org/10.1096/fj.202100539RR